

A Comparative Analysis on Inter-frequency Data Quality of Quad-constellation GNSS on a Smartphone

Yanjie Li Changsheng Cai*

School of Geosciences and Info-Physics, Central South University, Changsha 410083, People's Republic of China

* Corresponding author, cscai@hotmail.com

Abstract: This paper comprehensively analyzes the inter-frequency data quality of the quad-constellation Global Navigation Satellite System (GNSS) of GPS, GLONASS, BDS and Galileo on a smartphone. A series of indices, i.e. the number of visible satellites, data integrity rate, multipath, carrier-to-noise ratio (C/No), cycle-slip ratio and observation residuals, are employed to evaluate the data quality with a comparison between different constellations and frequencies. Experiments were conducted using the firstly released dual-frequency smartphone of Xiaomi Mi8. The results show that the GPS and BDS exhibit the best tracking performance in an open-sky environment with an average of 7 observed satellites at each epoch, which is 3 or 4 satellites more than the Galileo and GLONASS. In addition, the GPS data integrity rate is higher than the other constellations by about 20%-25%. The GPS suffers a multipath effect two times larger than the Galileo on the L1/E1 frequencies, but they are almost equal on the L5/E5a frequencies. For all four constellations, the C/No is mostly concentrated at 20-35 dB-Hz. Further, the C/No on the L1/E1 frequencies increases by 3-4 dB-Hz over the L5/E5a frequencies. The GLONASS observations exhibit the most serious cycle slip occurrence rate at a ratio of 100, which is significantly larger than the other constellations. Regarding the residuals, the phase RMS residuals for all four constellations are at a few millimeters, whereas the pseudorange residuals of GLONASS are

the most prominent with an RMS of over 6 m, which is 3-4 times larger than the other constellations. The precise point positioning (PPP) results show that the convergence time and positioning accuracy can be effectively improved by adding GPS and Galileo data at L5/E5a.

Key words: smartphone; GNSS; quad-constellation; inter-frequency; data quality

1. Introduction

Smartphones play an important role to promote the social and technical development in the age of mobile Internet. However, most smartphone applications depend on location information. In recent years, the demand for smartphone-based high-precision positioning services is increasing. In May 2016, Google announced to open the GNSS raw data interface for Android smartphones, which creates a condition for smartphone's high-precision positioning applications. However, most smartphones typically use linear polarized antennas due to limited space [1], resulting in degraded GNSS data quality when compared with the geodetic GNSS receivers, which largely restricts smartphones' positioning performance. Evaluating smartphones' GNSS data quality can aid to adopt appropriate strategies or develop suitable algorithms to reduce its negative effect.

Since the GNSS observation quality has a big impact on the positioning performance, the

smartphone GNSS data quality analysis has become a hot research subject. [2] firstly evaluated the raw GNSS observation quality on Android smart terminals and demonstrated that the pseudorange observations can only provide meter-level positioning accuracy, while the carrier-phase observations have the potential for centimeter-level positioning. [3] further compared the Nexus 9 tablet, Samsung Galaxy S8 smartphone and Huawei Honor v8 smartphone with the geodetic receiver in terms of the GNSS observation noise and concluded that the pseudorange observation noise of Nexus 9 is 10 times greater than the survey-grade receiver, while the carrier-phase observation noise is 3-5 times greater. By contrast, the observation noise of the latter two smartphones is much worse because of a duty-cycle issue. Meanwhile, smartphone observations are easily subject to gross errors [4]. Another major difference between the smartphone and geodetic receiver is the carrier-to-noise density ratio (C/No). The C/No of a smartphone is typically 10 dB-Hz lower than that of a geodetic receiver [2,5]. Meanwhile, the smartphone C/No varies rapidly even for the case at high satellite elevations [3]. Further, the smartphone C/No is more relevant to the pseudorange noise than the satellite elevation angles [6,7]. The duty cycle is a unique power-saving mechanism equipped in most smartphones. [7] and [4] show that the phase and pseudorange measurement inconsistency will increase and the accuracy of the doppler measurement will be reduced from cm/s to dm/s when the duty cycle mechanism is turned on. Fortunately, this mechanism can be turned off since the 9th version of the Android operating system was released in 2017 to acquire consecutive carrier-phase observations, which provides a possibility for carrier-phase-based high-precision positioning. Additionally, smartphone tests demonstrate that the linearly polarized antenna embedded inside smartphones is very sensitive to the multipath effect, which makes the multipath effect become a main error source in the smartphone-based GNSS positioning [8].

The integrated multi-frequency and multi-constellation GNSS positioning has become an

inevitable trend. Data quality is vital to determine the positioning performance. This study presents a comprehensive comparative analysis on inter-frequency and inter-constellation smartphone GNSS data quality. The Xiaomi Mi8 smartphone is used to collect the GNSS observations for a case study since it is the first one to support the dual-frequency and quad-constellation GNSS signals. The data quality characteristics are comprehensively analyzed by means of indices such as the number of visible satellites, data integrity rate, multipath effect, carrier-to-noise ratio, cycle-slip ratio and observation residuals.

2. Methodology

The data integrity rate is capable of reflecting the lack rate of GNSS data, and thus it is usually used to assess smartphones' GNSS signal reception capability. The data integrity rate can be expressed as a ratio of the actual received data (A_j^s) against the theoretical received data (T_j^s):

$$Ratio_j^s = A_j^s / T_j^s \quad (1)$$

where s and j denote the satellite and frequency, respectively. The theoretical reception data is calculated based on the satellite elevation mask angle and broadcast ephemeris [9].

The multipath effect is a major error source in the smartphone-based positioning. The multipath effect at an epoch (M_i) can be estimated using the multipath combination [10,11]:

$$M_i = P_i - \frac{f_i^2 + f_j^2}{f_i^2 - f_j^2} \varphi_i \lambda_i + \frac{2f_j^2}{f_i^2 - f_j^2} \varphi_j \lambda_j \quad (2)$$

where i and j ($i \neq j$) denotes two different frequencies. P is the pseudorange observation. φ is the carrier-phase observation. λ is the wavelength at the corresponding frequency f . M_i contains multipath effect, ambiguity term and hardware delay biases. The latter two items are stable and thus can be obtained by calculating the mean value of M_i at 15 consecutive epochs free of cycle slips [9], which is denoted as \bar{M}_i . Therefore, the multipath effect (MP_i) can be derived as:

$$MP_i = M_i - \bar{M}_i \quad (3)$$

The cycle slip ratio (CSR) reflects the stability of the carrier phase observations. The more cycle slips occur, the more challenging to achieve high-precision positioning solutions. The CSR is defined as the number of cycle slips every 1,000 epochs to reflect the occurrence frequency of cycle slips, as seen in Eq. (4):

$$CSR = \frac{1000}{o/n} \quad (4)$$

where n is the number of epochs when cycle slips occur and o is the number of all observed epochs. The geometry-free (GF) combination method [12] and the Melbourne–Wübbena (MW) method [13,14] are jointly used to detect dual-frequency cycle slips,

$$\nabla P^{m,n} = \nabla \rho^{m,n} + \nabla dt_{orb}^{m,n} + c \cdot \nabla dt_r^{m,n} + \nabla dI^{m,n} + \nabla dT^{m,n} + \nabla \varepsilon_p^{m,n} \quad (5)$$

$$\lambda \nabla \varphi^{m,n} = \nabla \rho^{m,n} + \nabla dt_{orb}^{m,n} + c \cdot \nabla dt_r^{m,n} + \lambda \cdot \nabla N^{m,n} - \nabla dI^{m,n} + \nabla dT^{m,n} + \nabla \varepsilon_\varphi^{m,n} \quad (6)$$

where ∇ is the single difference operator and m, n denote the reference and non-reference satellites, respectively. P and φ represent the pseudorange and carrier-phase observation, respectively. ρ is the geometric range between the receiver and satellite. c is the light speed. d_{orb} and dt_r are the satellite orbital error and clock bias. dI , dT denote the ionospheric and tropospheric delay errors, respectively. λ is the carrier phase wavelength, N is the ambiguity term, and ε is the observation noise term.

Secondly, the three-order differences of $\nabla P^{m,n}(t)$ between epochs are further made to eliminate systemic biases [3]. To simplify the expression, we set $\nabla P^{m,n}(t) = SD(t)$. According to the error propagation law, the pseudorange observation noise is obtained below:

$$\varepsilon_p(t) = \frac{SD_p(t+3) - 3SD_p(t+2) + 3SD_p(t+1) - SD_p(t)}{2\sqrt{10}} \quad (7)$$

Similarly, the carrier phase observation noise can be obtained as:

$$\varepsilon_\varphi(t) = \frac{SD_\varphi(t+3) - 3SD_\varphi(t+2) + 3SD_\varphi(t+1) - SD_\varphi(t)}{2\sqrt{10}} \quad (8)$$

whereas the code minus phase method and the loss of lock indicator (LLI) are jointly used to detect the single-frequency cycle slips [15].

To extract the observation noise, a zero-baseline method is commonly used [10,16]. But for smartphones, the zero-baseline method is difficult to be applied due to the inseparable receiver and antenna. In this study, we employ the four-order differential method to analyze the noise of observations [17]. First, an inter-satellite differencing operation is made to eliminate the receiver clock offset by choosing the highest-elevation satellite as a reference satellite. The inter-satellite single differences of pseudorange and carrier phase observations are derived as:

3. Data quality analysis of smartphone GNSS observations

3.1 Data description

A Xiaomi Mi8 smartphone equipped with a Broadcom BCM47755 chip and a linear polarization antenna is used for data collection with an open-sky view in static mode. The station is located on the top of mining building at Central South University, China, as displayed in Figure 1. The observation was made on November 23, 2019 from GPS time 2:00 to 12:00 with a data sampling interval of 1 s. The software of Geo++ Rinx Logger (V2.1.3) is used to transform the raw data information into the standard RINEX 3.02 format data. The Xiaomi Mi8 smartphone can receive quad-constellation signals at the same time, including GPS, GLONASS, BDS, and Galileo, but dual-frequency data can only be acquired from GPS and Galileo L1/L5 and E1/E5a signals, and the rest observations are all single-frequency data. The received GNSS signals come from GPS satellites of BLOCK IIA, BLOCK IIR, BLOCK IIR-M and BLOCK IIF, GLONASS satellites of GLONASS-M and GLONASS-K1, BDS satellite of GEO (Geosynchronous Earth Orbit), IGSO (Inclined

Geosynchronous Satellite Orbit) and MEO (Medium Earth Orbit), and Galileo satellites of Galileo-1 and Galileo-2.

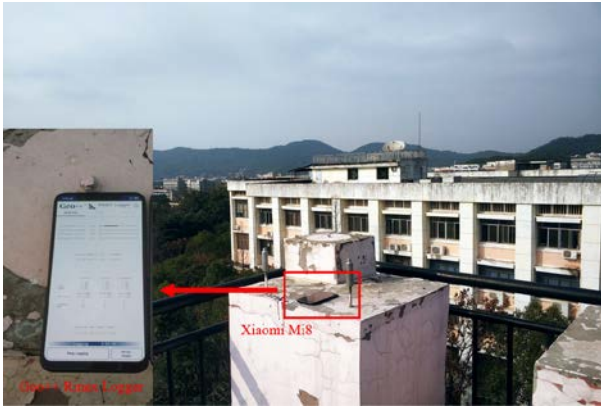


Figure 1 Smartphone data collection on the top of mining building at Central South University

3.2 GNSS signal reception capability analysis

Figure 2 shows the number of satellite observations for each satellite type and signal

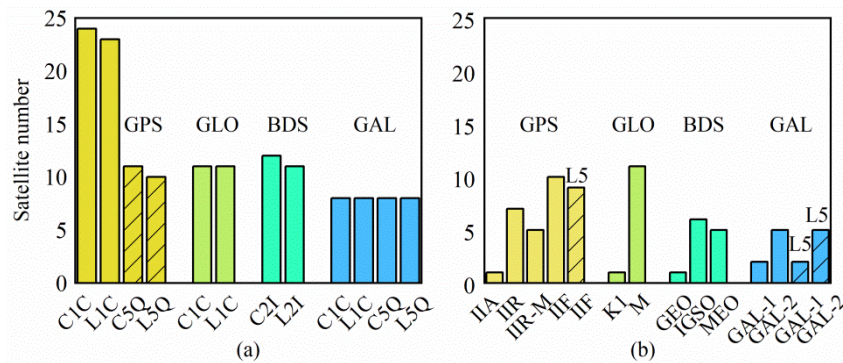


Figure 2 Number of observed satellites for different frequencies (a) and satellite types (b)

Figure 3 depicts the number of visible satellites for different constellations and frequencies during the entire observation period. On average, 7.8, 3.4, 7.5, and 3.5 satellites are tracked for GPS, GLONASS, BDS, and Galileo on the L1/G1/B1/E1 frequencies, and 2.5, 2.7 satellites are tracked for GPS and Galileo on the L5/E5a frequencies, respectively. It is obvious that an average of over 6 GPS and BDS satellites on the L1/B1 frequencies can be observed, while the observed Galileo and GLONASS satellite number on the E1/G1 frequencies is significantly less with an average of about 4. This demonstrates that the GPS and BDS satellites can be tracked more easily when compared with the Galileo and GLONASS satellites.

frequency. As can be seen from Figure 2(a), the Xiaomi Mi8 smartphone has the best ability to capture GPS signals. In the entire observation period, over 20 GPS satellites can be tracked. The GLONASS and BDS are followed with more than 10 satellites. It is noted that the carrier phase signal reception ability is slightly weaker than its pseudorange signal. In Figure 2(b), it is seen that only one BDS GEO satellite was observed, which suggests that the linearly polarized antenna is probably insensitive to the high-orbit GEO signals. Due to the limited number of GPS BLOCK IIF satellites, the observation number on the L5 frequency is almost half of those on the L1 frequency for GPS satellites. Unlike GPS, the numbers of the Galileo observations on the E1 and E5a frequencies are equal.

That is probably dependent on the GNSS chip and antenna embedded inside the smartphone. In addition, the average tracked numbers of GPS BLOCK IIF and Galileo satellites are 3.0 and 3.5 at each epoch on the L1/E1 frequencies, which are more than those on the L5/E5a frequencies by about 17% and 30%. This indicates that the Xiaomi Mi8 smartphone has a greater tracking ability for the L1/E1 signals than the L5/E5a signals.

The pseudorange and carrier phase data integrity rates for different constellations and frequencies during the entire observation period are listed in Table 1. The average data integrity rates for GPS/GLONASS/BDS/Galileo constellations are

60.3%, 37.6%, 38.2% and 35.5%, respectively. The results reveal that the GPS data integrity rate is 20%-25% higher than the other constellations. Meanwhile, the data integrity rate for the L5/E5a signals is obviously lower than the L1/E1 signals on the whole. Further, the carrier phase observations are more prone to missing data than the pseudorange observations, especially for L5/E5a signals. The maximum difference for different constellations exceeds 20%.

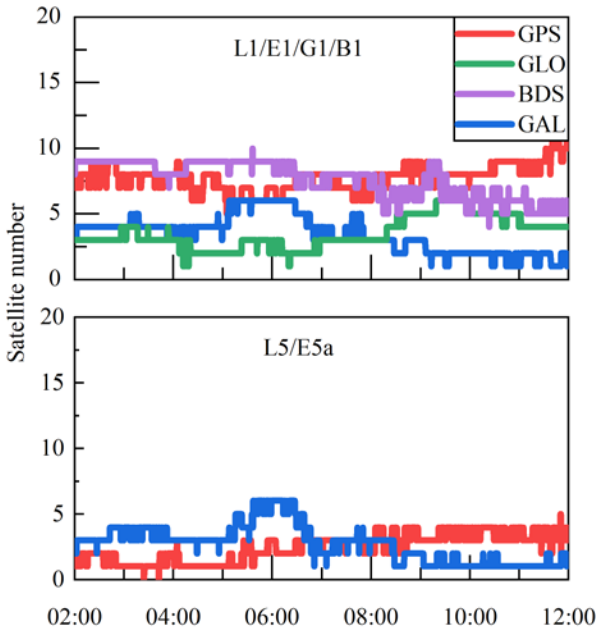


Figure 3 Number of visible satellites for different constellations and frequencies

Table 1 Data integrity rate of different observations for each frequency and constellation

Satellite type	Pseudorange		Carrier phase	
	L1/E1/G1/B	L5/E5	L1/E1/G1/B	L5/E5
	1	a	1	a
GPS	75.1	61.2	60.1	44.6
GLONAS S	40.2	-	35.0	-
BDS	42.9	-	33.5	-
Galileo	38.4	41.3	34.9	27.2

3.3 Analysis of C/No, multipath and cycle slip

Figure 4 depicts the frequency distribution histogram of the C/No at two different frequencies

and four different constellations. The corresponding RMS statistical values are also displayed in Figure 4. For a geodetic receiver, the C/No generally varies from 35 dB-Hz to 55 dB-Hz [4,7], while the C/No of the Xiaomi Mi8 smartphone is primarily concentrated at 20-35 dB-Hz for all constellations and frequencies, which is typically 15-20 dB-Hz lower than that of geodetic receivers. The C/No of the BDS B1, Galileo E5a, and GPS L5 signals are more concentrated below 30 dB-Hz while the C/No of the GLONASS G1, GPS L1 and Galileo E1 signals are mostly distributed in the range of over 30 dB-Hz. The C/No RMSs of four constellations on the L1/E1/G1/B1 differ less than 2 dB-Hz. Further, the C/No on the L1/E1 frequencies is stronger than that on the L5/E5a frequencies by over 3-4 dB-Hz, indicating that there exists a noticeable difference for the power of the signal at the two different frequencies.

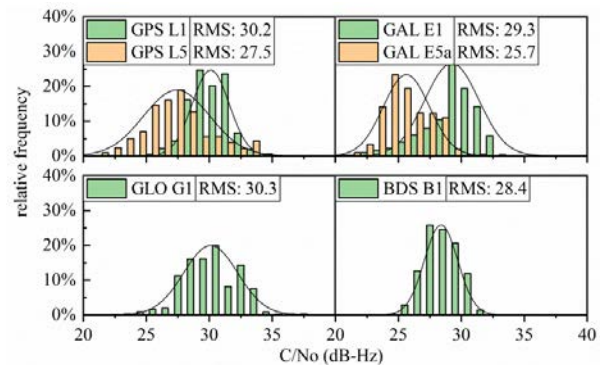


Figure 4 Frequency distribution histogram of carrier-to-noise ratio

Figure 5 shows the pseudorange multipath effects and the carrier phase cycle slip ratios. Based on Eq.(2) and Eq.(3), the pseudorange multipath effect of GPS and Galileo are acquired using dual-frequency observations and displayed in Figure 5 (a) along with its RMS statistical values. It is obvious that the GPS and Galileo pseudorange multipath RMSs are about 2.1 m and 1.3 m on the L1/E1 frequencies, and 0.6 m and 0.7 m on the L5/E5a frequencies, which are nearly 10 times larger than that of the geodetic receivers in an open area [18]. Further, the GPS pseudorange multipath effect is almost two times larger than the Galileo on the L1/E1 frequencies. For both constellations of GPS and Galileo, the pseudorange multipath effect is larger on the L1/E1 frequencies than the E1/E5a frequencies by about 71%

and 46%, respectively.

Figure 5 (b) shows the cycle-slip ratio for four constellations. Although the cycle slip detection is insensitive to single-frequency small cycle slips, the GLONASS observations still are found to contain cycle slips at over 100 epochs every 1,000 epochs. By contrast, the cycle slip ratio for geodetic receivers is usually less than 10 [19], indicating that the smartphone GLONASS observations are susceptible to lock-lose. On the contrary, the BDS has the lowest cycle-slip ratio at about 14 as compared to the other constellations.

constellations. Their corresponding RMS residuals statistical values with respect to different satellite types are listed in Table 2. Part epochs' residuals are not displayed as inter-satellite single-difference operation cannot be made due to the number of satellites is less than two.

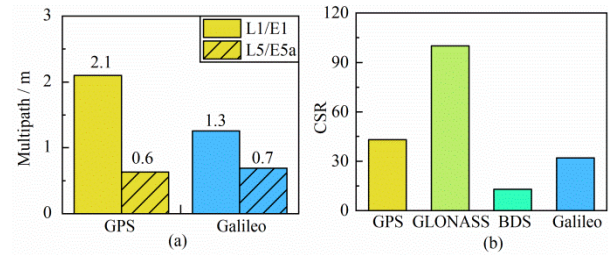


Figure 5 Pseudorange multipath effects (a) and carrier phase cycle slip ratio (b)

3.4 Analysis of observation residuals

The pseudorange and carrier-phase observation residuals can well reflect the observation quality. Figures 6 and 7 show the sequences of pseudorange and carrier phase observation residuals for different

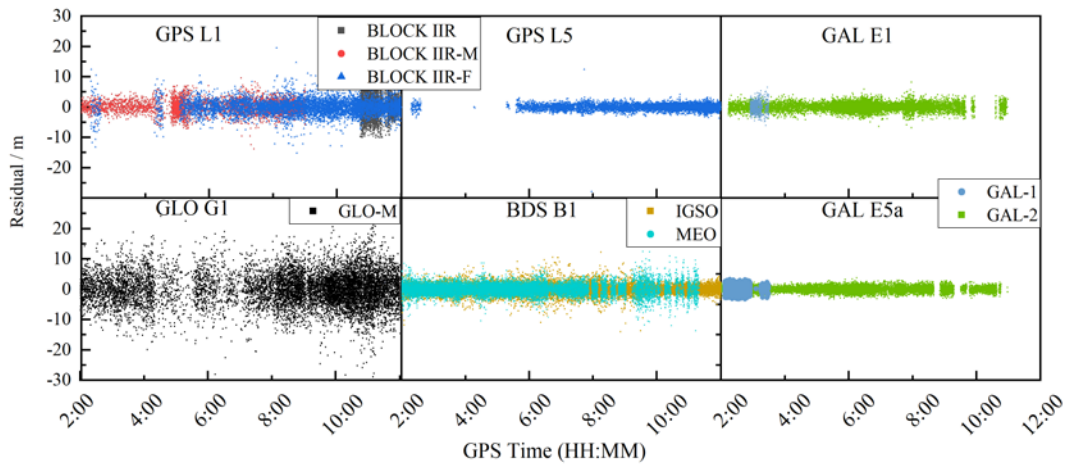


Figure 6 Pseudorange observation residuals for different GNSS constellations

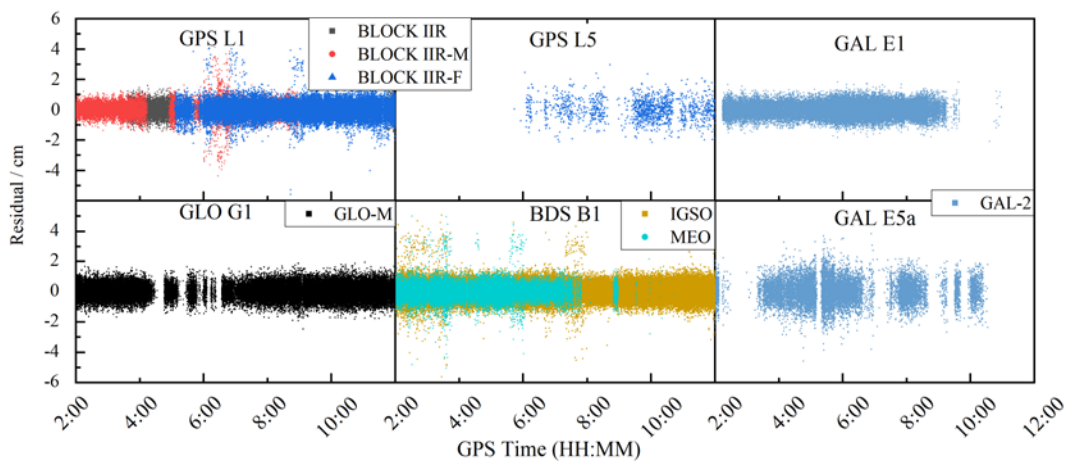


Figure 7 Carrier phase observation residuals for different GNSS constellations

Table 2 RMS statistics of pseudorange residuals and carrier phase residuals

	Satellite type	Pseudorange / m		Carrier phase / cm	
		L1/E1/G1/B1	L5/E5a	L1/E1/G1/B1	L5/E5a
GPS	BLOCK IIA	-	-	-	-
	BLOCK IIR	2.45	-	0.49	-
	BLOCK IIR-M	2.23	-	0.46	-
	BLOCK IIF	2.54	0.90	0.49	0.76
Galileo	GAL-1	2.32	1.08	-	-
	GAL-2	1.21	0.88	0.43	0.78
GLONASS	GLO_K1	-	-	-	-
	GLO_M	6.18	-	0.49	-
BDS	GEO	-	-	-	-
	IGSO	1.63	-	0.52	-
	MEO	1.70	-	0.47	-

According to Figure 6 and Table 2, it is apparently that the GPS and Galileo pseudorange observation accuracies on the L5/E5a frequencies are better than those on the L1/E1 frequencies. The GPS pseudorange RMS residuals on the L1 frequency are approximately twice larger than those on the L5 frequency. Galileo exhibits the highest pseudorange observation precision among all four constellations. Its RMS residuals are less than 1.5 m on the E1 frequency and 1 m on the E5a frequency. However, its signal reception capability is relatively poor, resulting in inadequate pseudorange observation data. As compared to the other constellations, the GLONASS pseudorange observations have the lowest precision with a RMS residuals of over 6 m, which is 3-4 times larger than the other constellations, probably attributing to its frequency division multiple access mode [10]. The Galileo pseudorange precision varies significantly from different satellite types, while it is not the case for the other constellations.

In contrast to the pseudorange observation residuals, the carrier phase observation precision on the L5/E5a frequencies is approximately 3-4 mm

lower than that of the L1/E1 frequencies. Meanwhile, the carrier observation precision varies little between different constellations as well as various satellite types with a RMS residuals value of about 5 mm.

4. Results of smartphone-based precise point positioning (PPP)

PPP is a high-precision positioning technique without a need of any reference station, which is very suitable for smartphone-based GNSS positioning. Because most smartphones can only generate single-frequency GNSS data, the single-frequency (SF) method is widely applied. This section compares the dual-frequency-PPP (DF-PPP) and the SF-PPP performance. Undifferenced and uncombined PPP model is adopted due to a large number of single-frequency data [20]. In the DF-PPP scenario, all dual-frequency data and single-frequency data are used. The SF-PPP scenario uses only the first-frequency data. Global Ionospheric Map (GIM) products are treated as pseudo-observables to reduce the effect of ionospheric errors on the single-frequency observations [8]. Satellite phase center offsets (PCO) and phase center variations (PCV) from International GNSS Service (IGS) are corrected and smartphone PCO is corrected using the recommended value from the reference [21]. The cut-off elevation is set to 10°. A C/No-dependent observation weighting method [22] is applied instead of the elevation-angle-dependent weighting method.

The experiment data is the same as in section 3.1. A known point is located near the smartphone at a distance of only a few centimeters. Thus, the coordinates of the known point can be used as references. The observation period is forced to reset the filter into 4 sessions with a session length of 2.5 hours for the sake of statistical computation of the convergence time and positioning accuracy. The position filter is considered to be converged when the positioning errors reach ± 1 m and keep within ± 1 m, and the positioning error is calculated using root mean square (RMS) after convergence. Figure 8 shows the PPP errors in the east, north and up directions using the DF-PPP and SF-PPP models in

four sessions. The DF-PPP model can converge to 1 m within 20 minutes in most sessions in the east and north directions, while the convergence time of the SF-PPP is about 2-3 times longer when compared to the DF-PPP. The convergence time of DF-PPP is improved about 68%, 69% and 53% when compared to the SF-PPP in east, north and up directions, respectively. Regarding the positioning accuracy, the DF-PPP RMS errors in all sessions reach 0.35 m,

0.30 and 0.52 m in the east, north and up directions, which improves the positioning accuracy by 24%, 27% and 20% over the SF-PPP model, respectively. In conclusion, the convergence time and positioning accuracy can be effectively improved by adding the observations on the L5/E5a frequency.

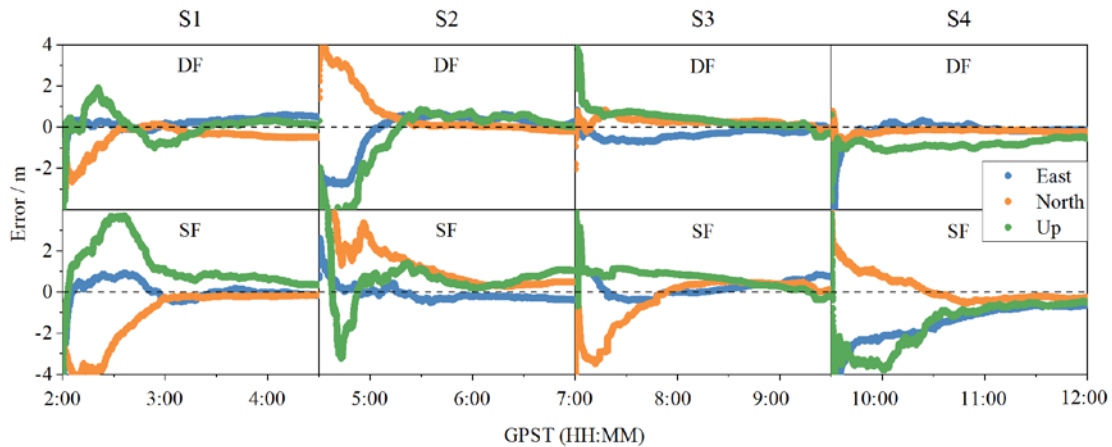


Figure 8 Positioning errors using DF-PPP and SF-PPP models in the east, north and up directions ('S' denotes 'Session')

5. Conclusions

The GNSS observation data quality is a key factor to determine the smartphone positioning performance. This manuscript comprehensively analyzes the smartphone GNSS data quality characteristics on two frequencies and four constellations based on the first released dual-frequency Xiaomi Mi8 smartphone. The data quality is evaluated through a series of indices such as signal reception capability, multipath, carrier-to-noise ratio, cycle-slip ratio, and observation residuals. Finally, the smartphone-based PPP positioning results are also presented.

The analysis results indicate that the GPS and BDS satellites have the best tracking performance with an average of up to 7 satellites per epoch, which is 3-4 more than the other constellations. The GNSS observation on the L1/E1 frequencies has a stronger signal reception ability than that on the L5/E5a frequencies. The GPS data integrity rate is 20%-25% higher than the other constellations, and the data integrity rate for the L5/E5a signal is obviously lower

than the L1/E1 signal. In addition, the C/No on the L1/E1 frequencies is stronger than that on the L5/E5a frequencies by over 3-4 dB-Hz. The C/No RMSs of four constellations on the L1/E1/G1/B1 frequencies differ slightly less than 2 dB-Hz. The GPS multipath effect is nearly two times larger than that of the Galileo on the L1/E1 frequencies, but they are almost equal on the L5/E5a frequencies.

The results also indicate that the GLONASS has the highest cycle slip ratio among all four constellations, while the BDS has the lowest cycle slip ratio. Similarly, the GLONASS has the largest pseudorange observation RMS residuals at over 6 m, which is 3-4 times higher than those of the other constellations. For all constellations and frequencies, the carrier phase residual precision is at a few millimeters and varies slightly from constellations and frequencies. It should be noted that all conclusions are achieved based on the used Xiaomi Mi8 smartphone. More types of smartphone data quality evaluation will be made in the future.

The positioning results demonstrate that the PPP convergence time can be improved by about 68%, 69%

and 53% in the east, north and up directions, and the positioning accuracy can be improved by about 24%, 27% and 20% after adding the observations on the L5/E5a frequencies to the first-frequency GNSS observations, respectively.

Acknowledgment:

The financial support from the National Key Research and Development Program of China (No. 2020YFA0713501), the National Natural Science Foundation of China (No. 42174040), the Hunan Natural Science Foundation (No.2020JJ4111), and the Hunan Provincial Innovation Foundation for Postgraduate (No. CX20200241) are appreciated.

References:

- [1] Pesyna K M, Heath R W, Humphreys T E. Centimeter positioning with a smartphone-quality GNSS antenna. Proceedings of ION GNSS+ 2014, Tampa, Florida, 8-12 September 2014, pp. 1568-1577.
- [2] Banville S, Van Diggelen F. Precise positioning using raw GPS measurements from Android smartphones. *GPS World*, 2016, 27(11): 43-48.
- [3] Li G , Geng J . Characteristics of raw multi-GNSS measurement error from Google Android smart devices. *GPS Solutions*, 2019, 23(3).
- [4] Liu W, Shi X, Zhu F, et al. Quality analysis of multi-GNSS raw observations and a velocity-aided positioning approach based on smartphones. *Advances in Space Research*, 2019, 63(8): 2358-2377.
- [5] Riley S, Lentz W, Clare A. On the path to precision-observations with android GNSS observables. Proceedings of the 30th International Technical Meeting of The Satellite Division of The Institute of Navigation (ION GNSS+ 2017). 2017: 116-129.
- [6] Zhang X , Tao X , Zhu F , et al. Quality Assessment of GNSS observations from an Android N smartphone and positioning performance analysis using time-differenced filtering approach. *GPS Solutions*, 2018, 22(3):70.
- [7] Paziewski J, Sieradzki R, Baryla R. Signal characterization and assessment of code GNSS positioning with low-power consumption smartphones. *GPS Solutions*, 2019, 23(4): 98.
- [8] Wang G, Bo Y, Yu Q, et al. Ionosphere-constrained single-frequency PPP with an Android smartphone and assessment of GNSS observations. *Sensors*, 2020, 20(20): 5917.
- [9] Vaclavovic P, Dousa J. G-Nut/Anubis: Open-source Tool for multi-GNSS data monitoring with a multipath detection for new signals, frequencies and constellations. *IAG 150 Years*. Springer, Cham, 2015: 775-782.
- [10] Cai C, He C, Santerre R, et al. A comparative analysis of measurement noise and multipath for four constellations: GPS, BeiDou, GLONASS and Galileo. *Survey review*, 2016, 48(349): 287-295.
- [11] Li B, Zang N, Ge H, et al. Single-frequency PPP models: analytical and numerical comparison. *Journal of Geodesy*, 2019, 93(12): 2499-2514.
- [12] Blewitt G. An automatic editing algorithm for GPS data. *Geophysical research letters*, 1990, 17(3): 199-202.
- [13] Melbourne W. The case for ranging in GPS-based geodetic systems. *Proc. 1st int. symp. on precise positioning with GPS*. 1985: 373-386.
- [14] Wubbena G. Software developments for geodetic positioning with GPS using TI 4100 code and carrier measurements. Proceedings 1st international symposium on precise positioning with the global positioning system. US Department of Commerce, 1985: 403-412.
- [15] Zhao J, Hernández-Pajares M, Li Z, et al. High-rate Doppler-aided cycle slip detection and repair method for low-cost single-frequency receivers. *GPS Solutions*, 2020, 24(3): 1-13.
- [16] Amiri-Simkooei A R , Tiberius C C J M . Assessing receiver noise using GPS shortbaseline time series. *GPS Solutions*, 2007, 11(1): 21-35.
- [17] Pirazzi G, Mazzoni A, Biagi L, et al. Preliminary

performance analysis with a GPS+Galileo enabled chipset embedded in a smartphone. Proceedings of ION GNSS+ 2017, Portland, Oregon, 25-29 September 2017, pp. 101-115.

- [18] Cai C, Gao Y, Pan L, et al. An analysis on combined GPS/COMPASS data quality and its effect on single point positioning accuracy under different observing conditions. *Advances in Space Research*, 2014, 54(5): 818-829.
- [19] Li J., Wang J., Xiong X., et al. Quality checking and analysis on GPS data in northeast asia. *Geomatics and Information Science of Wuhan University*, 2006(03): 209-212.
- [20] Zhou F, Dong D, Li W, et al. GAMP: An open-source software of multi-GNSS precise point positioning using undifferenced and uncombined observations. *GPS Solutions*, 2018, 22(2): 1-10.
- [21] Wanninger L., Heßelbarth A. GNSS code and carrier phase observations of a Huawei P30 smartphone: Quality assessment and centimeter-accurate positioning. *GPS Solutions*, 2020, 24(2), 1-9.
- [22] Wang L, Li Z, Wang N, et al. Real-time GNSS precise point positioning for low-cost smart devices. *GPS Solutions*, 2021, 25(2): 1-13.

Authors



Yanjie Li is currently working towards the M.D. degree in Surveying and Mapping Science and Technology in the School of Geosciences and

Info-physics, Central South University, China. His research focus on the smartphone-based GNSS precise point positioning.



Changsheng Cai is currently a Professor in the School of Geosciences and

Info-physics at the Central South University, Changsha, China. His current research interests include GNSS Precise Point Positioning and atmospheric error modeling.